thermochemically more stable isomer **1** which eventually emerges as the only "detectable" isomer. In our experiment, **1** and **2** are also simultaneously generated with a range of little excess energy. Due to the high barriers for isomerization or (direct)[19] dissociation, the isomer F_3N-H^+ (**2**) is trapped in a deep potential well; hence, it will not give rise to a metastable ion decomposition. In contrast, a portion of the fluorine-protonated isomer F_2N-FH^+ has enough internal energy to undergo time-delayed dissociation to NF_2^+ and HF. As indicated in Figure 2, the energy necessary to bring about this process is <14.6 kcal mol^{-1}. If one takes into account the contribution of the thermal energy of the system, this energy demand is provided for part of the F_2N-FH^+ ion population in the protonation NF_3 with CH_5^+. Most importantly, as there is no reverse activation energy and the excess energy is small, a metastable ion peak with a small kinetic energy release results, as shown in Figure 3B.

A fundamentally different situation prevails if H_3^+ is used in the protonation of NF_3. Again, first principle considerations suggest that the proton will be transferred to either site of NF_3; i.e., both F_2N-FH^+ (**1**) and F_3N-H^+ (**2**) will be formed. However, in contrast to the reaction employing CH_5^+, the internal energy of the so-formed ions **1** and **2** will be much higher. This has two implications. (i) Most of the fluorine-protected ions will already dissociate in the ion source, and only a small, low-energy fraction will have a lifetime such that dissociation in the second or third field-free region will occur. Consequently, the fraction of this process to the composite peak (narrow component of Figure 3A) is quite small. (ii) F_3N-H^+ is now formed with internal energy high enough that a portion can overcome the barrier imposed by the transition structure **3**[19] to eventually dissociate (from vibrationally/rotationally excited **1**) to NF_2^+ and HF. In view of previous findings,[5,13,18] it is not unreasonable to argue that the tight transition structure **3** and the large energy difference between **3** and the products NF_2^+/HF (ca. 39 kcal mol^{-1}) result in the dished-top peak as shown in Figure 3A. It goes without saying that, based on the potential energy surface depicted in Figure 2, a more refined picture will emerge by performing appropriate ion/trajectory calculations.

In conclusion, the combined theoretical/experimental approach employed in this study demonstrates that both the fluorine and the nitrogen protonated form of NF_3 are distinct species in the gas phase. Both ions are separated by a significant barrier (52.6 kcal mol^{-1}) which prevents facile interconversion. The global minimum corresponds to the fluorine protonated isomer F_2N-FH^+ (**1**), which can be viewed as an ion/dipole complex. The nitrogen-protonated form F_3N-H^+ (**2**) is 6.4 kcal mol^{-1} less stable. While the former isomer has a low-energy dissociation channel to produce NF_2^+ and HF (theory, 14.6 kcal mol^{-1}; experimental data, 10.9 kcal mol^{-1}), the isomer F_3NH^+ (**2**) is trapped in a deep potential well, which prevents both rapid isomerization and dissociation. It is this particular aspect of the potential energy surface which explains the different kinetic energy releases (KER's) data obtained from the dissociation of **1** and **2**: HF loss from F_2N-FH^+ (**1**) gives rise to a small KER (21 meV, Figure 3B), while the same reaction of F_3NH^+ (**2**) is associated with a dished-top peak (Figure 3A) and a large KER (740 meV).

Acknowledgment. The generous financial support of our work by the Fonds der Chemischen Industrie, the Deutsche Forschungsgemeinschaft, and the Gesellschaft von Freunden der Technischen Universität Berlin is gratefully appreciated. F.G. is indebted to the Consiglio Nazionale delle Richerche (CNR) of Italy for a visiting fellowship.

(19) It was not possible to locate a transition structure for the *direct* elimination of HF from F_3N-H^+ (**2**).

Conformational Analysis. 15. 1,2-Dibromotetrafluoroethane and 1,2-Diiodotetrafluoroethane. Electron Diffraction Investigations of the Molecular Structures, Compositions, and Anti–Gauche Energy and Entropy Differences

Hanne Thomassen, Svein Samdal,† and Kenneth Hedberg*

Contribution from the Department of Chemistry, Oregon State University, Corvallis, Oregon 97331. *Received September 17, 1991*

Abstract: The molecular structures and conformational compositions of 1,2-dibromotetrafluoroethane (DBTF) and 1,2-diiodotetrafluoroethane (DITF) have been investigated in the gas phase by electron diffraction each at three nozzle-tip temperatures: DBTF, 273, 388, and 673 K; DITF, 293, 393, and 473 K. Both molecules exist as a mixture of anti and gauche rotamers with the former the more stable. Distances (r_g/Å) and angles ($\angle_\alpha$/deg) for the lowest temperatures, with estimated 2σ uncertainties, are as follows: (DBTF) r(C–F) = 1.340 (3), r(C–C) = 1.559 (13), r(C–Br) = 1.930 (5), ∠CCF = 109.9 (4), ∠FCF = 108.4 (8), ∠CCBr = 110.5 (5), and ∠BrCCBr$_G$ = 67 (3); (DITF) r(C–F) = 1.334 (3), r(C–C) = 1.542 (13), r(C–I) = 2.146 (7), ∠CCF = 109.1 (6), ∠FCF = 108.2 (7), ∠CCI = 111.7 (6), and ∠ICCI$_G$ = 70 (3). The rotameric compositions of DBTF at 273, 388, and 673 K were found to be 30 (8), 39 (14), and 53 (18) % gauche, from which the energy and entropy differences are calculated to be $E°_G - E°_A$ = 3.6 (11) kJ/mol and $S°_G - S°_A + R \ln 2$ = 6.0 (34) J/(mol·K). For DITF at 298, 393, and 473 K, the compositions are 19 (6), 24 (11), and 35 (13) % gauche from which the energy and entropy differences are $E°_G - E°_A$ = 5.1 (15) kJ/mol and $S°_G - S°_A + R \ln 2$ = 5.0 (44) J/(mol·K). The structures and thermodynamic properties are discussed.

Introduction

Ethanes substituted in the 1,2 positions exist as mixtures of anti and gauche conformers as a result of rotation around the C–C bond. In the dihalogenated ethanes 1,2-dichloro-,[1] 1,2-dibromo-,[2] and 1,2-diiodoethane,[3] the predominance of the anti over gauche can be explained by steric effects. In 1,2-difluoroethane the gauche

† Present address: Oslo College of Engineering, Cort Adelers gt. 30, N-0254, Oslo 2, Norway.

(1) Kveseth, K. *Acta Chem. Scand., Ser. A* **1975**, *29*, 307. Kveseth, K. *Ibid.* **1974**, *28*, 482.
(2) Kveseth, K. *Acta Chem. Scand. Ser. A* **1978**, *32*, 63.
(3) Samdal, S.; Hedberg, K. Unpublished results.

0002-7863/92/1514-2810$03.00/0

form is the more stable[4] by reason of the "gauche effect".[5] Recent ab initio work on 1,2-difluoroethane indicates that the gauche preference does not result from fluorine-atom attraction, but instead from the formation of "bent bonds":[6] for the C–C bond, the hybrid orbital from each carbon atom does not point at the other center, but at a small angle away from it. In the anti form the two bond components are thus parallel to each other; in the gauche form, however, they tend to point toward each other and achieve better overlap.

Destabilization of the anti forms by fluorine atoms in the 1,2 positions raises the question of the many differences in other haloethanes. For example, in the molecules 1,2-dibromotetrafluoroethane (hereafter DBTF) and 1,2-diiodotetrafluoroethane (DITF), steric repulsion between the two bromine or iodine atoms is expected to favor the anti form. According to the bent bond concept, fluorine substitution should lower the anti–gauche energy difference compared to 1,2-dibromo- and 1,2-diiodoethane.

Both DBTF and DITF have been investigated by IR and Raman spectroscopy in solid, solution, liquid, and gas phase, and it is known that in the liquid and gas phases each exists in anti and gauche conformations with anti the more stable.[7-12] These studies provide estimates of the anti–gauche energy differences,[8-10] assignments of most of the fundamental vibrational frequencies for each conformer, and normal coordinate analyses.[11,12] There have also been studies of the photoelectron spectra of both molecules[13] and for DBTF acoustic[9] and powder neutron diffraction studies as well.[14] There remain structural and conformational questions about both molecules, however, and we decided to carry out electron-diffraction investigations of them.

Experimental Section

Materials. The samples of both DBTF and DITF were obtained from PCR Inc. GC/MS analysis showed that the liquid sample of DBTF contained about 7 mol % acetone. DBTF and acetone have nearly the same boiling point from which one expects about the same mole ratio in the vapor. The low scattering of acetone relative to DBTF was judged to be insignificant at this level and the sample was used as received. GC analysis showed that the purity of the DITF sample was greater than 98%; it was also used as received.

Apparatus and Procedure. All diffraction photographs were made with the Oregon State apparatus fitted with an r^3 sector. Nominal nozzle-to-plate distances were 750 mm (longer camera) and 300 mm (shorter camera). The diffraction patterns on 8 × 10 in. Kodak projector slide plates (medium contrast) were developed 10 min. in D-19 developer diluted 1:1.

For DBTF other experimental conditions were as follows: nozzle-tip temperatures, 273, 388, and 673 K; ambient apparatus pressure during exposures, (4.0–5.8) × 10^{-6} Torr; exposure times, 60–200 s; beam currents, 0.33–0.42 μA; nominal electron wavelength, 0.049 Å; wavelength calibration against CS_2 in a different experiment with r_a(C=S) = 1.557 Å and r_a(S···S) = 3.109 Å. Analyses of the data at each temperature were based on three plates from the longer camera distance, and two (298 and 388 K) and three (673 K) plates from the shorter distance. Data in the ranges $2.00 \le s/Å^{-1} \le 16.00$ (longer camera) and $9.00 \le s/Å^{-1} \le 38.50$ (shorter camera) in intervals $\Delta s = 0.25$ Å^{-1} were obtained.

The pictures of DITF were taken and analyzed in 1974, and retraced and reanalyzed in 1989 to make use of improvement in microdensitometric equipment. Experimental conditions were as follows: nozzle-tip temperatures, 298, 393, and 473 K; ambient apparatus pressure during exposures (1.6–4.6) × 10^{-6} Torr; exposure times, 20–210 s; beam current

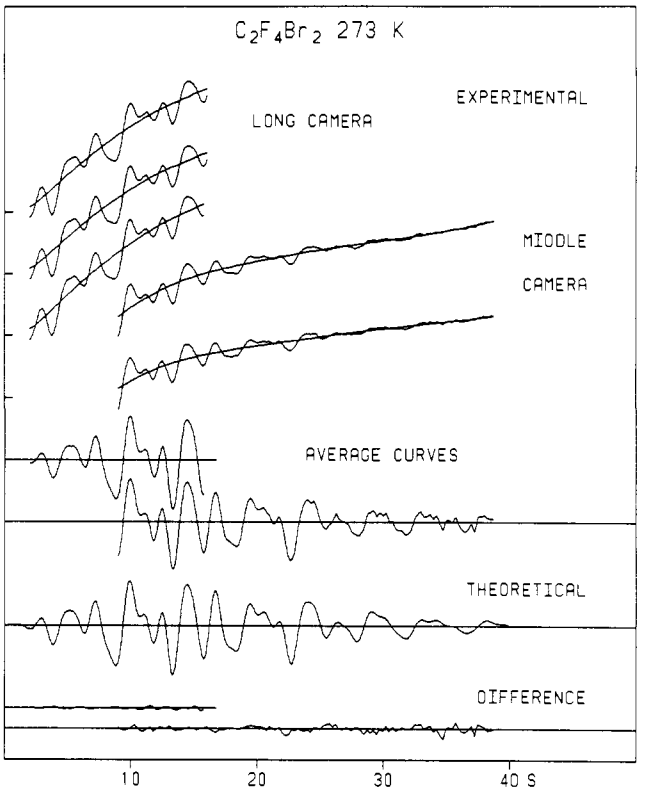

Figure 1. Intensity curves for dibromotetrafluoroethane at 273 K. The s^4I_t experimental curves are shown magnified seven times with respect to the backgrounds on which they are superimposed. The average curves are $s[s^4I_t - \text{bkgd}]$. The theoretical curve is calculated from parameter values given in Table I.

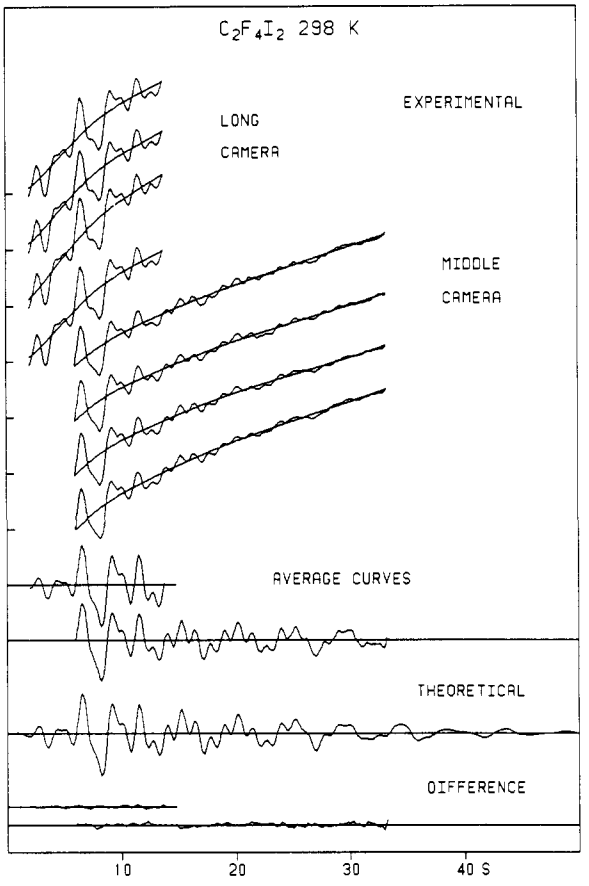

Figure 2. Intensity curves for diiodotetrafluoroethane at 298 K. See legend to Figure 1.

(4) Friesen, D.; Hedberg, K. *J. Am. Chem. Soc.* **1980**, *102*, 3987.
(5) See, e.g.: Wolfe, S. *Acc. Chem. Res.* **1972**, *5*, 102.
(6) Wiberg, K. B.; Murcko, M. A.; Laidig, K. E.; MacDougall, P. J. *J. Phys. Chem.* **1990**, *94*, 6956.
(7) Glockler, G.; Sage, C. J. Chem. *Phys.* **1941**, *9*, 387.
(8) Kagarise, R. E.; Daasch, L. W. *J. Chem. Phys.* **1955**, *23*, 130.
(9) Crook, K. R.; Park, P. J. D.; Wyn-Jones, E. *J. Chem. Soc. A* **1969**, 2910.
(10) Serboli, G.; Minasso, B. *Spectrochim. Acta, Part A* **1968**, *24*, 1813.
(11) Shurvell, H. F.; Cahill, F.; Devarajan, V.; James, D. W. *Can. J. Chem.* **1976**, *54*, 2220.
(12) Powell, D. L.; Gustavsen, J. E.; Klaeboe, P.; Nielsen, C. J. *J. Raman Spectrosc.* **1978**, *7*, 111.
(13) Chau, F. T.; McDowell, C. A. *J. Phys. Chem.* **1976**, *80*, 2923.
(14) Powley, G. S.; Whitley, E. *Acta Crystallogr. C* **1988**, *44*, 1249.

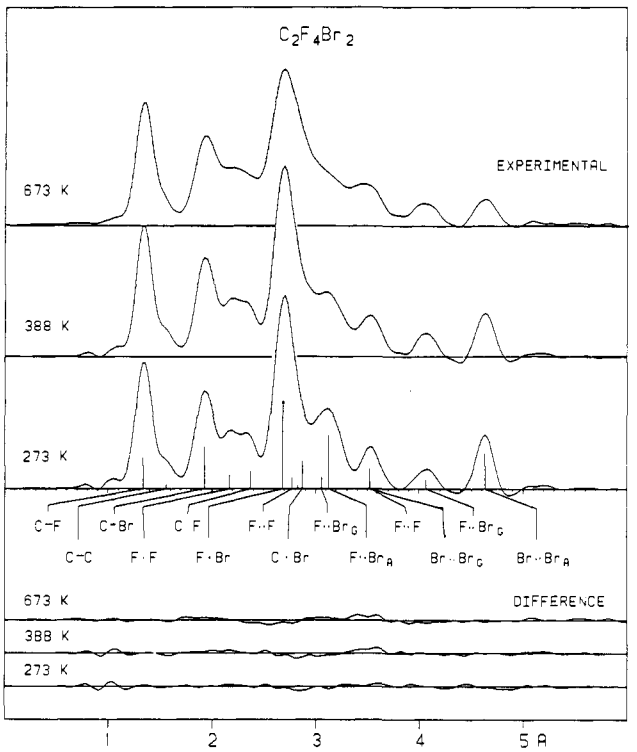

Figure 3. Radial distribution curves for dibromotetrafluoroethane. The experimental curves were calculated from composites of the average intensities with use of theoretical data for the region $0 \le s/Å^{-1} \le 1.75$, and $B/Å^2 = 0.0025$. The vertical lines indicate the interatomic distances and have lengths proportional to the distance weights.

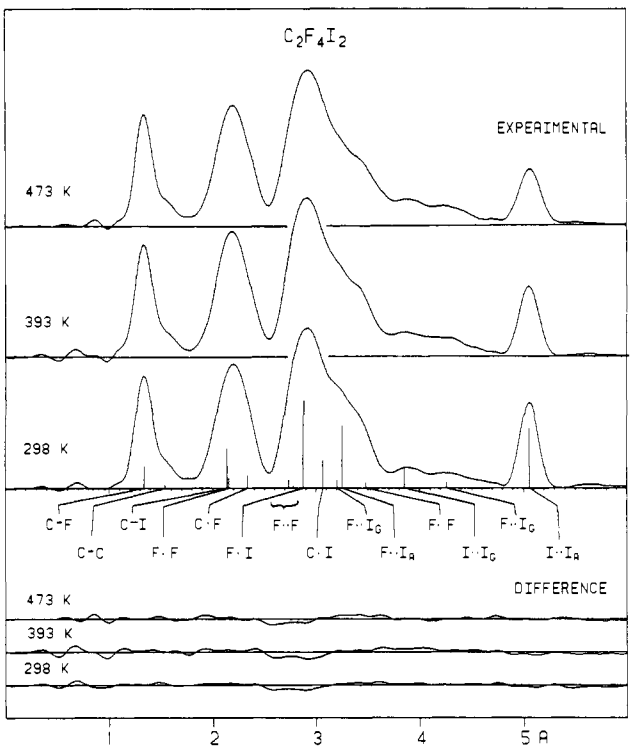

Figure 4. Radial distribution curves for diiodotetrafluoroethane. See legend to Figure 3.

0.38–0.42 μA; nominal electron wavelength, 0.058 Å; wavelength calibration against CO_2 in a separate experiment with $r_a(CO) = 1.1646$ Å and $r_a(O\cdots O) = 2.3244$ Å. Analyses of the data at each temperature were based on four plates from the longer, and four (298 K), and three (393 and 473 K) plates from the shorter camera distance. Data in the ranges $2.00 \le s/Å^{-1} \le 13.50$ and $6.00 \le s/Å^{-1} \le 33.50$ at intervals $\Delta s = 0.25$ Å^{-1} were obtained from these experiments.

The procedures for obtaining the scattered intensity distribution have been described.[15,16] The electron-scattering amplitudes and phases were obtained from tables.[17] Figures 1 and 2 show curves of the total scattered intensities and the final backgrounds for the experiments on each molecule at the lowest experimental temperature. The corresponding curves for the other temperatures and the data for the average curves are available as supplementary material. Total intensity data and the calculated backgrounds are available from the authors.

Radial distribution curves $rD(r)$, were calculated in the usual way by Fourier transformation of functions $I'_m(s) = sI_m(s)Z_C Z_F A_C^{-1} A_F^{-1} \exp(-Bs^2)$ with B equal to 0.0015 Å^2 for the DBTF data and 0.0020 Å^2 for the DITF. Theoretical intensity curves were used for the unobserved region $s < 2.00$ Å^{-1}. The experimental $rD(r)$ curves for all temperatures are seen in Figures 3 and 4. There are striking changes in these curves as the experimental temperature is increased. The peaks broaden significantly due to the larger amplitude of vibration at highest temperatures (this is particularly true for DBTF), and some peaks change in area. The latter changes reveal immediately that the anti form of the molecules is the more stable. For DBTF the peaks at 4.6 and 3.5 Å are due to the Br···Br distances in the anti and gauche forms, respectively, and, as the experimental temperature increases, the peak at 3.5 Å increases in area at the expense of the one at 3.5 Å, indicating conversion of the anti to gauche. For DITF the circumstance is similar, but less striking because of the smaller temperature range, for the peaks at 5.0 and 3.9 Å.

Structure Analysis. Force Field Calculations. Because the vibrational spectra of both conformers of each molecule have been assigned and normal coordinate analyses carried out, it was a simple task to take account of the effects of vibrational averaging ("shrinkage"). This was done by defining the structure in terms of r_α distances. These are related to the r_a distance consistent with the diffraction experiment according to $r_a - r_\alpha = \delta r + K - l^2/r$. The first two terms on the right are corrections due to centrifugal distortion and to amplitudes of vibration perpendicular to the line of atomic centers, and may be calculated from a harmonic force field. The last term involves the mean-square amplitude of vibration which may be either calculated or given the experimental value. For the calculations we used the program ASYM20[18] to symmetrize the internal force constants,[11,12] to adjust the symmetrized force field to fit the observed fundamental wavenumbers to within 1 cm^{-1} (the unobserved torsional frequency for the anti form of DBTF were taken from ref 9), and finally to calculate the correction terms.

Models of the Structures and Refinement Results. In earlier studies of substituted ethanes different models comprising substantial amounts of anti and gauche conformers, several different models have been used to represent the system. These models, designated 2C ("two conformer"), 2S ("double sigma"), and CP ("cosine potential") have been described in detail in a previous article in this series.[4] Each of these models was tested in the case of DBTF. It was found that the 2S model yielded very small values of the root-mean-square amplitude of the torsion angle (with increasing temperature the values were σ_{anti}/deg = 2.6 (11), 3.4 (18), and 6 (3) and σ_{gauche}/deg = 3.8 (18), 3 (4), and 5 (3)). The narrow potential minimum represented by these values implies that the simple 2C model, which represents all vibrations to be of the "frame" type, would be a satisfactory description of the system. Although a similar test for DITF was not done, a similar result is surely to be expected. As for most other systems in this series, we assumed that the structures of the conformers for each molecule differ only in their torsional angle. The set of parameters common to the conformers was chosen to be the distances (X = I or Br) r(C–X), $\langle r(C–C,F)\rangle = (4/5)r(C–F) + (1/5)r(C–C)$, $\Delta = r(C–F) - r(C–C)$, and the angles ∠CCX, ∠CCF, and ∠FCF. Specification of the gauche form required one more parameter, a torsion angle ∠(XCCX). The composition parameter of the system was represented by the mole fraction of the gauche form, X_G. In the refinement of the structure of DBTF we included acetone as an impurity. The structure of and a force field for acetone, which allowed us to calculate vibrational quantities, were taken from an ab initio calculation.[19]

Some of the many vibrational parameters (amplitudes) could be refined individually; others were handled in the usual way by combining

(15) (a) Gundersen, G.; Hedberg, K. *J. Chem. Phys.* **1969**, *51*, 2500. (b) Hagen, K.; Hedberg, K. *J. Am. Chem. Soc.* **1973**, *95*, 1003.
(16) Hedberg, L. *Abstracts*, Fifth Austin Symposium on Gas Phase Molecular Structure, Austin, TX, March 1974; p 37.
(17) (a) Elastic amplitudes and phases: Ross A. W.; Fink, M; Hilderbrant, R. *International Tables for Crystallography*; International Union of Crystallography; Reidal, Dordrecht, in press. (b) Inelastic amplitudes: Cromer, D. T.; Mann, J. B. *J. Chem. Phys.* **1967**, *47*, 1892. Cromer, D. T. *Ibid.* **1969**, *50*, 4857.
(18) Hedberg, L. *Abstracts*, Seventh Austin Symposium on Gas Phase Molecular Structure, Austin, TX, Feb 1978; p 49.
(19) Boggs, J. E. Unpublished results.

Table I. Results for Structure-Defining Parameters of 1,2-Dibromo- and 1,2-Diiodotetrafluoroethane[a]

	$C_2F_4Br_2$			$C_2F_4I_2$		
	273 K	388 K	673 K	298 K	393 K	473 K
$\langle r$(C-F,C)$\rangle$[b]	1.379 (3)	1.376 (4)	1.368 (5)	1.371 (3)	1.366 (5)	1.371 (3)
Δr[c]	0.233 (14)	0.213 (18)	0.190 (23)	0.211 (14)	0.201 (24)	0.226 (19)
r(C-X)	1.925 (5)	1.925 (7)	1.925 (9)	2.139 (7)	2.144 (11)	2.143 (10)
∠CCX	110.5 (5)	110.7 (8)	111.6 (13)	111.7 (6)	111.6 (10)	111.5 (9)
∠CCF	109.9 (4)	110.0 (6)	110.6 (8)	109.1 (6)	109.4 (10)	109.3 (12)
∠FCF	108.4 (8)	108.3 (12)	107.7 (16)	108.2 (7)	107.8 (10)	108.6 (9)
$\angle XCCX_G$[d]	67 (3)	67 (5)	69 (7)	70 (3)	69 (5)	69 (5)
X_G[e]	30 (8)	39 (14)	53 (18)	19 (6)	25 (11)	35 (13)
R[f]	0.12	0.15	0.17	0.10	0.15	0.14

[a] Distances (r_α) in ångströms and angles ($\angle_\alpha$) in degrees. [b] Equal to (4/5)r(C-F) + (1/5)r(C-C). [c] Equal to r(C-F) − r(C-C). [d] Torsion angle in gauche form. [e] Mole fraction of gauche form. [f] Quality of fit factor equal to $[\sum w_i\Delta_i^2/w_i(s_iI_i(\text{obsd}))^2]^{1/2}$, where $\Delta_i = s_iI_i(\text{obsd}) - s_iI_i(\text{calcd})$.

Table II. Distances (r/Å) and Amplitudes (l/Å) for 1,2-Dibromotetrafluoroethane[a,b]

	273 K			388 K			673 K		
	r_α	r_g	l	r_α	r_g	l	r_α	r_g	l
				common to anti and gauche					
C-F	1.334 (3)	1.340	0.052 } (4)	1.333 (3)	1.340	0.045 } (4)	1.330 (3)	1.340	0.053 } (4)
C-C	1.557 (13)	1.559	0.060 }	1.546 (17)	1.548	0.054 }	1.520 (23)	1.523	0.064 }
C-Br	1.925 (5)	1.930	0.051 (7)	1.925 (7)	1.932	0.050 (8)	1.925 (9)	1.937	0.069 (9)
$F_4 \cdot F_5$	2.165 (10)	2.171	0.062 } (6)	2.162 (16)	2.170	0.067 } (9)	2.147 (22)	2.162	0.079 } (13)
$C_1 \cdot F_7$	2.371 (8)	2.374	0.069 }	2.362 (12)	2.367	0.075 }	2.346 (18)	2.343	0.089 }
$F_4 \cdot Br_3$	2.676 (4)	2.682	0.067 } (5)	2.672 (5)	2.681	0.070 } (6)	2.657 (8)	2.672	0.104 } (9)
$C_1 \cdot Br_6$	2.869 (8)	2.873	0.073 }	2.864 (12)	2.869	0.077 }	2.857 (19)	2.866	0.113 }
	anti								
$F_5 \cdot F_T$	2.774 (12)	2.778	[0.106]	2.767 (17)	2.772	[0.123]	2.761 (2)	2.770	[0.158]
$F_4 \cdot Br_6$	3.123 (7)	3.128	0.110 (9)	3.120 (10)	3.127	0.131 (15)	3.125 (16)	3.137	0.185 (31)
$F_4 \cdot F_7$	3.519 (9)	3.521	0.054 (10)	3.511 (13)	3.514	0.067 (18)	3.498 (19)	3.502	0.083 (22)
$Br_3 \cdot Br_6$	4.631 (8)	4.633	0.077 (8)	4.629 (12)	4.631	0.083 (13)	4.629 (19)	4.632	0.106 (23)
	gauche								
$F_5 \cdot F_T$	2.71 (3)	2.71	[0.109]	2.70 (4)	2.71	[0.126]	2.68 (6)	2.69	[0.163]
$F_4 \cdot F_7$	2.82 (3)	2.82	[0.107]	2.82 (5)	2.83	[0.124]	2.83 (7)	2.85	[0.160]
$F_4 \cdot Br_6$	3.06 (4)	3.07	0.117 (9)[c]	3.05 (5)	3.06	0.139 (17)[c]	3.04 (7)	3.05	0.197 (31)[c]
$Br_3 \cdot Br_6$	3.52 (5)	3.52	0.146 } (10)[d]	3.52 (7)	3.53	0.182 } (18)[d]	3.57 (11)	3.58	0.240 } (23)
$F_4 \cdot F_8$	3.516 (9)	3.520	0.055 }	3.508 (18)	3.513	0.067 }	3.493 (18)	3.501	0.083 }
$F_5 \cdot Br_6$	4.066 (7)	4.068	0.067 (29)	4.060 (10)	4.063	0.068 (30)	4.052 (14)	4.058	0.108 (30)

[a] Quantities in parentheses are estimated 2σ. [b] Amplitudes in curly brackets were refined in groups; those in square brackets were calculated from the force field and were not refined. [c] Refined in group with $l(F_4 \cdot Br_6)$. [d] Refined in group with $l(F_4 \cdot F_7)$ in the anti form.

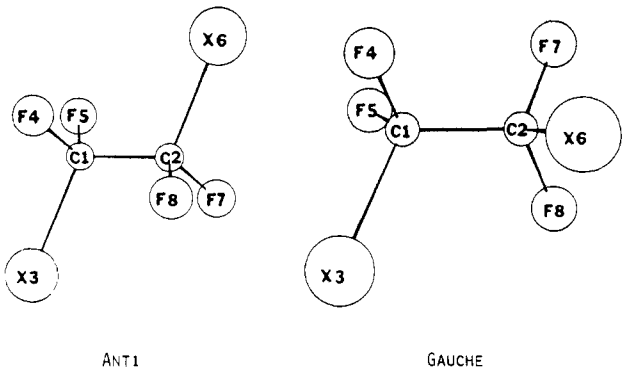

Figure 5. Diagrams of anti and gauche forms of dibromo- and diiodoethane.

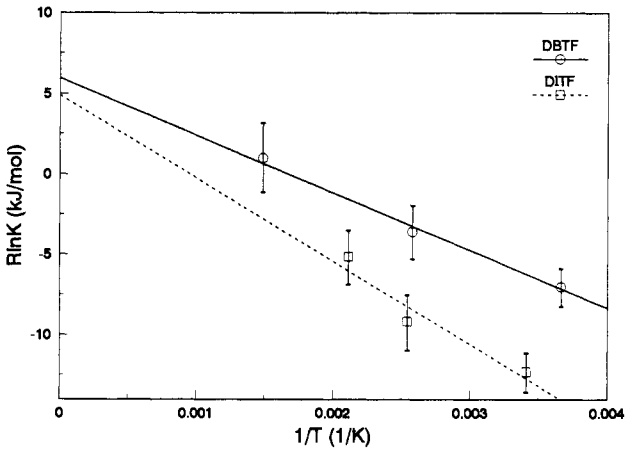

Figure 6. van't Hoff plot of the results for the rotameric composition of dibromo- and diiodotetrafluoroethane. The lines are least squares fits to the experimental data. The vertical bars are estimated 1σ.

them into groups. Differences among members of a group were taken from the results of calculations based on the force fields. The amplitude parameters used are evident from the tables of results. Atom numbering is shown in Figure 5.

The refinements were done by least squares fitting of the models to the average intensity curves from each camera distance.[20] The final results for the two molecules are given in Tables I–III. Table IV contains correlation matrices corresponding to the results for the geometrical parameters from the lowest temperature experiments; those for the higher temperatures are similar. Correlation matrices for all refined parameters from the lowest temperature experiments are given in the supplementary material.

(20) Hedberg, K.; Iwasaki, M. *Acta crystallogr.* **1964**, *17*, 529.

Discussion

Perhaps the most interesting feature of these systems is their thermodynamic properties. The quantities $\Delta E° = E°_G - E°_A$ and $\Delta S° = S°_G - S°_A$ may be determined from the usual formula R ln $(X_G/X_A) - R$ ln 2 = $-\Delta E°/T + \Delta S°$, where the statistical weight of the gauche form has been removed from $S°_G$. The results for DBTF are $\Delta E°$ = 3.6 (11) kJ/mol and $\Delta S° + R$ ln 2 = 6.0 (34) J/(mol·K) and for DITF $\Delta E°$ = 5.1 (15) kJ/mol and $\Delta S° + R$ ln 2 = 5.0 (44) J/(mol·K); van't Hoff plots of the data are seen in Figure 6. The energy differences are in good

Table III. Distances (r/Å) and Amplitudes (l/Å) for 1,2-Diiodotetrafluoroethane[a,b]

	298 K			393 K			473 K		
	r_α	r_g	l	r_α	r_g	l	r_α	r_g	l
				common to anti and gauche					
C–F	1.328 (3)	1.334	0.046 } (4)	1.326 (4)	1.333	0.047 } (5)	1.326 (3)	1.335	0.044 } (5)
C–C	1.540 (13)	1.542	0.052 }	1.527 (23)	1.530	0.054 }	1.552 (18)	1.555	0.051 }
C–I	2.139 (7)	2.146	0.057 } (10)	2.144 (11)	2.153	0.058 } (15)	2.143 (10)	2.154	0.057 } (13)
$F_4 \cdot F_5$	2.153 (9)	2.160	0.058 }	2.142 (13)	2.152	0.058 }	2.154 (12)	2.166	0.057 }
$C_1 \cdot F_7$	2.340 (9)	2.343	0.074 (12)	2.331 (17)	2.336	0.085 (21)	2.351 (16)	2.356	0.075 (16)
$F_4 \cdot I_3$	2.868 (6)	2.876	0.078 (7)	2.869 (12)	2.880	0.083 (12)	2.865 (14)	2.878	0.101 (14)
$C_1 \cdot I_6$	3.063 (8)	3.068	0.09 (2)	3.055 (13)	3.062	0.110 (7)	3.072 (13)	3.080	0.102 (18)
	anti								
$F_5 \cdot F_7$	2.734 (13)	2.739	0.118 (8)[c]	2.731 (21)	2.738	0.130 (12)[c]	2.742 (24)	2.750	0.151 (14)[c]
$F_4 \cdot I_6$	3.256 (9)	3.262	0.137 } (12)	3.249 (17)	3.256	0.148 } (18)	3.271 (22)	3.281	0.179 } (28)
$F_4 \cdot F_7$	3.479 (11)	3.482	0.066 }	3.471 (18)	3.475	0.062 }	3.487 (21)	3.491	0.082 }
$I_5 \cdot I_6$	5.054 (7)	5.056	0.079 (5)	5.052 (10)	5.054	0.089 (10)	5.065 (12)	5.068	0.101 (4)
	gauche								
$F_5 \cdot F_7$	2.62 (3)	2.62	0.115 } (7)[c]	2.62 (5)	2.63	0.126 } (12)[c]	2.64 (5)	2.65	0.147 } (15)[c]
$F_4 \cdot F_7$	2.81 (3)	2.81	0.109 }	2.80 (6)	2.81	0.118 }	2.81 (7)	2.83	0.139 }
$F_4 \cdot I_6$	3.17 (3)	3.17	0.132 } (13)[d]	3.17 (6)	3.17	0.142 } (19)[d]	3.18 (6)	3.19	0.172 } (28)[d]
$F_4 \cdot F_8$	3.475 (10)	3.480	0.066 }	3.468 (17)	3.474	0.062 }	3.482 (17)	3.490	0.082 }
$I_5 \cdot I_6$	3.87 (5)	3.87	0.14 (4)	3.84 (8)	3.85	0.17 (6)	3.86 (9)	3.87	0.18 (6)
$F_5 \cdot I_6$	4.251 (8)	4.254	0.054 (41)	4.246 (12)	4.250	0.058 (51)	4.261 (12)	4.266	0.117 (94)

[a] Quantities in parentheses are estimated 2σ. [b] Amplitudes in curly brackets were refined in groups; those in square brackets were calculated from the force field and were not refined. [c] Refined in group with $l(F_4 \cdot I_3)$. [d] Refined in group with $l(F_4 \cdot I_6)$ in the anti form.

Table IV. Correlation Matrices (×100) for 1,2-Dibromo- and 1,2-Diiodotetrafluoroethane[a]

parameter	σ(DBTF)[b]	σ(DITF)[b]	r_1	r_2	r_3	$\angle_4$	$\angle_5$	$\angle_6$	$\angle_7$	X_8
1. $\langle r$(C–F,C)$\rangle$[c]	0.09	0.09	100	−49	54	<1	−47	18	23	−13
2. r(C–X)	0.18	0.23	−47	100	−28	−57	62	40	−29	<1
3. Δr[c]	0.48	0.49	58	−36	100	−38	−63	48	19	−2
4. $\angle$(CCX)	18.5	19.7	6	−75	−24	100	−27	−67	14	−6
5. $\angle$(CCF)	15.9	20.8	−42	81	−51	−53	100	−25	−20	−11
6. $\angle$(FCF)	28.0	24.2	15	26	51	−59	−7	100	−7	6
7. $\angle$XCCX[d]	107.7	99.3	14	−21	5	20	−23	−18	100	−31
8. X_G[e]	2.98	2.21	12	10	−15	−6	3	−11	14	100

[a] Coefficients for DBTF and DIBF are respectively above and below the diagonal. [b] Standard deviations (×100) from least squares: distances (r) an ångströms; angles ($\angle$) in degrees. [c] See footnotes to Table I. [d] Torsional angle in the gauche form. [e] Mole fraction of the gauche form.

agreement with values obtained from gas-phase vibrational spectroscopy: DBTF, 3.2 (21) kJ/mol;[8] DITF, 6.8 (42) kJ/mol.[10] Since the bent bonds invoked to account for the greater stability of the gauche form of 1,2-difluoroethane arise from the presence of the very electronegative fluorine atoms, one might expect bent bonds to play a role in DBTF and DITF. However, because both bromine and iodine are more electronegative than hydrogen, it may be supposed that the bond paths between the carbon atoms more nearly coincide with the lines joining the atomic centers. Steric repulsion between pairs of bromine or iodine atoms coupled with the reduced tendency for bent-bond stabilization of the gauche forms thus accounts for the greater stability of the anti. The CCX angles, larger than in 1,2-difluoroethane, are consistent with smaller bond bendings. Likewise, the larger conformational energy difference in DITF relative to DBTF is consistent with greater steric repulsion in DITF.

Our structural analyses made use of the simplifying assumption that the structures of the two conformers of each molecule differed only in their torsion angles. The results of ab initio calculations on similar species suggest that bond-length differences are unlikely to exceed 0.005 Å and bond-angle differences 3°. To the extent that the assumption is incorrect, all distances and angles represent weighted averages for the two forms. The assumption is unlikely to affect significantly the values deduced for the thermodynamic properties.

Variation in the bond lengths of halogen-substituted hydrocarbons is usually explained in terms of electrostatic effects combined with rehybridization of the carbon orbitals. Thus, the electronegative halogens attract electrons preferentially from the carbon p orbitals, which leads to increased s character and thus to shorter lengths for all the bonds to that carbon atom. At the same time the resulting (positive) charges on the carbons tend to lengthen the C–C bonds. As the following comparisons show, our results for DBTF and DITF are consistent with this picture. The C–F and C–C bond lengths (r_g) in 1,1,2,2-tetrafluoroethane are respectively 1.351 (2) Å and 1.520 (5) Å,[21] and in hexafluoroethane 1.326 (2) Å and 1.545 (6) Å.[22] The effects just mentioned are expected to be smaller in the former, and larger in the latter, than in either DBTF or DITF. The r_g values of C–F in DBTF and DITF lie between those cited. One would also expect the C–C distances to be intermediate between those in 1,1,2,2-tetrafluoro- and hexafluoroethane, and, although this is formally trure for DITF, the large uncertainties associated with the values of r_g(C–C) in both DITF and DBTF rule out quantitative comparisons.

The van der Waals distances for F···F, F···Br, Br···Br, F···I, and I···I are respectively 3.04, 3.5, 3.9, 3.6, and 4.3 Å. From Tables II and III it is seen that the interatomic distances between halogen atoms which are gauche to each other are smaller than the corresponding van der Waals distances by 0.2–0.6 Å. Torsional movement near the potential minima shortens some of these distances and increases the nonbond repulsion. The small root-mean-square amplutides of the torsional motion in these molecules find ready explanation in these facts. The average values of the torsion angles (for DITF slightly greater than for DBTF, but both larger than 60°) are consistent with a minimization of van der Waals repulsion.

Acknowledgment. This work was supported by the National Science Foundation under Grant CHE88-10070.

Registry No. DBTF, 124-73-2; DIFT, 354-65-4.

(21) Brown, D. E.; Beagly, B. *J. Mol. Struct.* **1977**, *38*, 167. The r_a values given in the article have been converted to r_g for comparison purposes.
(22) Gallaher, K. L.; Yokoseki, A.; Bauer, S. H. *J. Phys. Chem.* **1974**, *78*, 2389. See also: Swick, D. A.; Karle, I. L. *J. Chem. Phys.* **1955**, *23*, 1499.

Supplementary Material Available: Tables of average molecular intensities for each camera distance at each temperature, symmetry coordinates, force constants, observed and calculated wavenumbers, and correlation matrices for all refined parameters at the lowest temperature experiments and figures of total intensities with backgrounds for experiments at 388 K and 673 K (DBTF) and 393 K and 473 K (DITF) (16 pages). Ordering information is given on any current masthead page.

Direct Observation of Epinephrine and Norepinephrine Cosecretion from Individual Adrenal Medullary Chromaffin Cells

Edward L. Ciolkowski, Bruce R. Cooper, Jeffrey A. Jankowski, James W. Jorgenson, and R. Mark Wightman*

Contribution from the Department of Chemistry, University of North Carolina, Chapel Hill, North Carolina 27599-3290. *Received October 15, 1991*

Abstract: Cyclic voltammetry at Nafion-coated carbon fiber microelectrodes has been used to monitor directly the release of catecholamines from individual adrenal medullary chromaffin cells and to identify the released catecholamine as epinephrine or norepinephrine. The cultured cells were induced to secrete by exposure to 100 μM nicotine, a recognized secretagogue at these cells. Each cell contains on average 167 fmol of catecholamines, and the secretion event involves only a small percentage of the total stores for a time interval of less than 60 s. Identification of epinephrine and norepinephrine is accomplished because of differences in the rates of intracyclization for the oxidized forms of these compounds which results in differences in the shapes of their voltammograms. Approximately 75% of the cells studied released only epinephrine or norepinephrine in response to a 100 μM nicotine stimulus, while 25% released mixtures of both catecholamines. The ratio of epinephrine:norepinephrine releasing cells is in good agreement with the epinephrine:norepinephrine ratios of total catecholamine stores for the cell populations. Analysis of individual cell catecholamine content by microcolumn liquid chromatography following secretion measurements indicates that the individual cells release catecholamines in the same proportions in which they store catecholamines.

Introduction

Isolated adrenal medullary chromaffin cells in culture are frequently used as a model system for neurosecretion.[1-4] It is generally accepted that at least two subpopulations of adrenal cells exist: those which store and secrete epinephrine (E) and those which store and secrete norepinephrine (NE). This conclusion has been arrived at on the basis of the results of electron microscopy studies which showed two principal types of adrenal cells differing in the size and electron density of their catecholamine storage vesicles,[2,5-8] referred to as granules, and enzyme assays which showed that a subpopulation of cells lacked phenylethanolamine *N*-methyltransferase (PNMT), the enzyme which converts norepinephrine into epinephrine.[9] Some data also suggest that differences in certain aspects of release for these two cell types exist.[10,11] A recent report has shown that these subpopulations can be separately isolated with their secretory machinery still intact.[12]

The majority of studies on adrenal cells have been performed on populations of cells because of experimental limitations. However, techniques are now available which allow for analysis at the level of the single cell. To accomplish this, femtomole and lower detection limits are required. Microcolumn liquid chromatography and capillary zone electrophoresis provide a means to precisely sample the contents of individual cells.[13-16] However, these methods lack sufficient time resolution to monitor a dynamic event such as exocytosis. Recently, microelectrodes have been used to provide spatial and temporal information on local chemical events, a technique referred to as scanning electrochemical microscopy.[17-19] This laboratory has recently used these approaches to monitor secretion of catecholamines from individual adrenal cells in culture with subsecond time resolution.[20,21] Although this technique has provided sufficient time resolution to accurately describe the local changes in catecholamine concentrations at the cell surface, identification of the specific catecholamine secreted has not been possible.

The goal of the present study has been to identify the specific catecholamine secreted, epinephrine or norepinephrine, while the dynamic process of cellular release is monitored. Identification is based on known differences in the rates of intracyclization for

* To whom correspondence should be addressed.

(1) Burgoyne, R. D. *Biochim. Biophys. Acta* **1991**, *1071*, 174-202.
(2) Livett, B. G. *Pharmacol. Rev.* **1984**, *64*, 1103-1161.
(3) Trifaro, J. M.; Lee, R. W. H. *Neuroscience* **1980**, *5*, 1533-1546.
(4) Fenwick, E. M.; Fajdiga, P. B.; Howe, N. B. S.; Livett, B. G. *J. Cell Biol.* **1978**, *76*, 12-30.
(5) Hillarp, N. A.; Hockfelt, B. *Acta Physiol. Scand.* **1953**, *30*, 55-68.
(6) Eranko, O. *Acta Anat.* **1962**, *16*, 1-60.
(7) Coupland, R. E.; Kobayashi, S. In *Chromaffin, Enterochromaffin and Related Cells*; Coupland, R. E., Fujita, T., Eds.; Elsevier Scientific Publishing Co.: New York, 1976; Chapter 6.
(8) Terland, O.; Flatmark, T.; Kryvi, H. *Biochim. Biophys. Acta* **1979**, *553*, 460-468.
(9) Moro, M. A.; Lopez, M. G.; Gandia, L.; Michelena, P.; Garcia, A. G. *Anal. Biochem.* **1990**, *185*, 243-248.
(10) Kilpatrick, D. L.; Ledbetter, F. H.; Carson, K. A.; Kirshner, A. G.; Slepetis, R.; Kirshner, N. *J. Neurochem.* **1980**, *35*, 679-692.
(11) Marley, P. D.; Livett, B. G. *Neurosci. Lett.* **1987**, *77*, 81-86.
(12) Moro, M. A.; Garcia, A. G.; Langley, O. K. *J. Neurochem.* **1991**, *57*, 363-369.
(13) Kennedy, R. T.; Oates, M. D.; Cooper, B. R.; Nickerson, B.; Jorgenson, J. W. *Science* **1989**, *246*, 57-63.
(14) Kennedy, R. T.; Jorgenson, J. W. *Anal. Chem.* **1989**, *61*, 436-441.
(15) Oates, M. D.; Cooper, B. R.; Jorgenson, J. W. *Anal. Chem.* **1990**, *62*, 1573-1577.
(16) Olefirowicz, T. M.; Ewing, A. G. *Anal. Chem.* **1990**, *62*, 1872-1876.
(17) Bard, A. J.; Fan, F. F.; Pierce, D. T.; Unwin, P. R.; Wipf, D. O.; Zhou, F. *Science* **1991**, *254*, 68-74.
(18) Bard, A. J.; Denuault, G.; Lee, C.; Mandler, D.; Wipf, D. O. *Acc. Chem. Res.* **1990**, *23*, 357-363.
(19) Engstrom, R. C.; Pharr, C. M. *Anal. Chem.* **1989**, *61*, 1099A-1104A.
(20) Leszczyszyn, D. J.; Jankowski, J. A.; Viveros, O. H.; Diliberto, E. J., Jr.; Near, J. A.; Wightman, R. M. *J. Biol. Chem.* **1990**, *265*, 14736-14737.
(21) Leszczyszyn, D. J.; Jankowski, J. A.; Viveros, O. H.; Diliberto, E. J., Jr.; Near, J. A.; Wightman, R. M. *J. Neurochem.* **1991**, *56*, 1855-1863.

0002-7863/92/1514-2815$03.00/0